



## ORIGINAL ARTICLE

# Osteogenic potential of human dental pulp stem cells, and human dermal fibroblasts exposed hydroxyapatite nanoparticles: A comparative in vitro study

Mohsen Naseri<sup>1#</sup> , Sepideh Sarfi<sup>2,3#</sup> , Mohammad Yahya Hanafi-Bojd<sup>4,5</sup> , Ehsaneh Azaryan<sup>5\*</sup>

1. Cellular and Molecular Research Center, School of Medicine, Birjand University of Medical Sciences, Birjand, Iran
2. Student Research Committee, Birjand University of Medical Sciences, Birjand, Iran
3. Department of Immunology, School of Medicine, Birjand University of Medical Sciences, Birjand, Iran
4. Department of Pharmaceutics and Pharmaceutical Nanotechnology, School of Pharmacy, Birjand University of Medical Sciences, Birjand, Iran
5. Cellular and Molecular Research Center, Birjand University of Medical Sciences, Birjand, Iran

## ARTICLE INFO

**Received:** 2025/01/28

**Revised:** 2025/03/12

**Accepted:** 2025/03/16

**DOI:**

#These authors contributed equally to this work

\*Corresponding:

Ehsaneh Azaryan

**Address:**

Cellular and Molecular Research Center, Birjand University of Medical Sciences, Birjand, Iran

**E-mail:**

Ehsaneh.Azaryan@gmail.com

## ABSTRACT

This study aimed to evaluate the osteogenic response of human dermal fibroblasts (hDFs) and human dental pulp stem cells (hDPSCs) when exposed to hydroxyapatite nanoparticles (HA-NPs), which are commonly employed biomaterials in the field of bone regeneration. The sol-gel method was employed to synthesize HA-NPs. Cell viability was assessed using the MTT assay after 24 and 72 hours of exposure to HA-NPs. Osteogenic differentiation was assessed through Alizarin red S staining (ARS), alkaline phosphatase (ALP) activity assay, and quantitative real-time PCR (qPCR) to evaluate the expression levels of osteogenic markers, including BMP-2, VEGF-A, RUNX2, and IL-6. The HA-NPs had a nanorod shape, with dimensions of 17–29 nm in width and 62–89 nm in length. Both hDPSCs and hDFs demonstrated enhanced osteogenic potential when exposed to HA-NPs, as indicated by increased ARS staining for calcium deposition and elevated ALP activity. Gene expression analysis showed up-regulation of BMP-2 and VEGF-A and down-regulation of RUNX2 in both cell types. IL-6 expression markedly increased in hDFs but did not show significant changes in hDPSCs compared to the control group. The findings of this study suggest that HA-NPs may enhance the osteogenic capability of hDPSCs and hDFs. The results demonstrate that while fibroblasts exhibit some mineralization potential, hDPSCs are the most suitable cell type for bone regenerative applications.

**Keywords:** Stem cell, Fibroblast, Hydroxyapatite, Nanoparticle, Bone regeneration



© The Author(s).

Publisher: Babol University of Medical Sciences

This work is published as an open access article distributed under the terms of the Creative Commons Attribution 4.0 License (<http://creativecommons.org/licenses/by-nc/4/>). Non-commercial uses of the work are permitted, provided the original work is properly cited.

## Introduction

Large bone defects, whether resulting from traumatic injuries, tumors, or infectious processes, necessitate external bone reconstruction (1). Autologous bone grafting stands out as the benchmark in bone graft material selection. This approach offers significant advantages due to its nonimmunogenic and histocompatible nature.

Conversely, the procurement of autografts is linked to issues such as donor site morbidity, blood loss, and potential chronic discomfort (2). In recent years, regenerative medicine and tissue engineering have developed as revolutionary areas, presenting groundbreaking strategies for producing new bone tissue to satisfy the requirements of skeletal restoration and bone augmentation. These strategies attempt to use stem cells, new scaffolds, and biological factors to develop, possibly, sturdy, repeatable, and increased bone creation procedures to improve an elderly population's quality of life (3).

To address bone tissue deficiency, the chosen biomaterial should facilitate cell migration and differentiation into bone cells. Additionally, local angiogenesis must take place to supply the nutrients and environmental conditions required for the proper development of the bone tissue (4). Current tendencies in biomaterials for bone regeneration have been centered around enhancing osteoinductive characteristics and the capacity to promote bone regeneration by utilizing calcium phosphates, particularly hydroxyapatite (HA) (5). HA constitutes the primary inorganic element present in human hard tissues and is extensively utilized in bone tissue engineering, owing to its exceptional biocompatibility, capacity to stimulate bone development, and its biological characteristics (6).

Moreover, it can increase the concentration of  $\text{Ca}^{2+}$  in the local area, thus promoting the proliferation of osteoblasts and facilitating the growth and differentiation of mesenchymal stem cells (MSCs) (7). MSCs are being researched for their potential to support bone tissue engineering by differentiating into osteoblasts and endothelial cells. Although this kind of stem cell is traditionally extracted from bone marrow (BMSCs), it may also be derived from a variety of neonatal and adult tissues, including dental pulp, orbicularis oris muscle, and fat. Many researches are focusing on the separation of MSCs from more

accessible sources, with the goal of making these cells safer to use in clinical settings for tissue engineering (4). Recently, human dental pulp stem cells (hDPSCs) have drawn interest as viable options for cell-based regenerative treatments. hDPSCs excel in mineralized matrix production compared to MSCs from adipose tissue or bone marrow, making them suitable for restoration of dental injuries or mandibular bone abnormalities (8-11).

In addition to stem cells, dermal fibroblasts represent a possible cell source that aligns with these criteria. Dermal fibroblasts can be readily obtained through a punch biopsy from the patient's skin and maintained up to passage 14 without experiencing any decrease in collagen biosynthesis or growth rate (12). Recent years have witnessed a growing interest in utilizing fibroblasts as a starting point for differentiation into various cell types, including osteoblasts (13). Many similarities exist between MSCs and fibroblasts in morphology, surface markers, gene expression, and potential for differentiation.

In vitro studies demonstrated that fibroblasts exhibit plastic adherence and the ability to differentiate into bone, fat, and cartilage while expressing key MSC surface markers. These distinctive characteristics position fibroblasts as promising candidates for clinical applications across a spectrum of diseases, offering a compelling alternative for regenerative purposes owing to their widespread obtainability and abundance (8, 14, 15). In this study, we evaluated the osteogenic response of human dermal fibroblasts (hDFs) and hDPSCs in vitro when exposed to hydroxyapatite nanoparticles (HA-NPs), a widely used biomaterial in bone tissue engineering.

## Methods

### Synthesis and characterization of HA-NPs

The HA-NP was synthesized following our previous study (11). Calcium nitrate tetrahydrate and diammonium hydrogen phosphate (both from Sigma-Aldrich, USA) were dissolved in deionized water with a 1.67 molar ratio. Calcium nitrate tetrahydrate solution was stirred at 50°C for 30 minutes. The diammonium hydrogen phosphate mixture was afterwards poured dropwise (1 mL/min) into the prepared solution. The pH was then raised to 11 with the addition of NaOH. After that, the mixture was stirred at 50°C for a duration of 90 minutes. Subsequent

to this, the mixture underwent centrifugation, followed by three washes with deionized water and ethanol. FTIR and XRD were employed to evaluate the functional groups and phase composition of HA-NPs respectively. SEM and TEM evaluated the generated nanoparticles morphological and structural characteristics (Additional file).

### Cell culture and osteogenic differentiation

hDPSCs were extracted from the healthy third molars of three individuals (aged 20–25) years at Imam Reza Hospital's Dental Center in Birjand, in compliance with the ethical standards of Birjand University of Medical Sciences (ethical number: IR.BUMS.REC.1399.090). The patient's agreement was obtained for this procedure. Previous research covered the characterization and isolation of hDPSCs (Additional file) (16). hDFs were acquired from the Iranian cell bank of the Pasteur Institute (NCBI Code: C646).

The cells were cultivated in DMEM (Gibco, Grand Island) supplemented with 10% FBS (Capricorn, South America) and 1% penicillin-streptomycin (Sigma-Aldrich, St. Louis, MO) and incubated at 37°C in 5% CO<sub>2</sub>. To induce osteogenic differentiation, cells were grown in osteogenic differentiation medium (OM) containing DMEM enriched with ascorbic acid (50 µM), β-glycerol phosphate (10 mM), and dexamethasone (10 nM) (all from Sigma-Aldrich/Merck, Germany), as discussed previously (17). The cells were cultured for 14 days in OM alone (control) and HA-NPs without OM. Subsequently, on the 14th day, the cells were collected and used for alizarin red S (ARS), alkaline phosphatase (ALP), and quantitative real-time PCR (qPCR) assays.

### Cell viability assay

The MTT test was utilized to determine the cytotoxic effect of HA-NPs on hDPSCs and hDFs. Initially, the cells were seeded at a density of 10<sup>4</sup> cells per well in a 96-well plate and allowed to adhere for 24 hours. Subsequently, the cells were exposed to varying concentrations of HA-NPs (0, 5, 10, 25, 50, and 100 µg/ml) for 24 and 72 hours. After removing the supernatant, 100 µl of DMSO was applied to every well. At 570 nm, a scanning spectrophotometer was used to measure the samples' optical absorbance (Biotek Epoch, Winooski, VT) (11).

### Alizarin red S assay

A 24-well plate was seeded with 5×10<sup>4</sup> hDPSCs and hDFs. When the cells reached 70% confluence, they were treated with HA-NPs, whereas the control group was left untreated. The positive control group included cells that had been exposed to OM. All cells underwent a 14-day culture cycle. The culture media was replenished every three days during the incubation phase. On day 14, the cells were rinsed with distilled water and then fixed in ice-cold 70% ethanol for 60 minutes. Subsequently, ARS dye (40 mM, pH 4.2) was used to stain the fixed cells, which were stained for 30 minutes at room temperature in darkness, the wells were rinsed with deionized water and immersed in 10% cetylpyridinium chloride solution to release calcium ions. Calcium deposition was evaluated by measuring the solution's absorbance at 540 nm (18).

### Alkaline phosphatase activity

hDPSCs and hDFs were planted at a density of 10<sup>5</sup> cells in a 12-well plate to evaluate alkaline phosphatase activity. The cells in the control group were treated with OM after they reached 70% confluence, whereas another group was exposed to HA-NPs without OM. On the 14th day of the experiment, supernatants were collected, and the manufacturer's procedure was followed to figure out the ALP activity in the collected supernatants using an ALP assay kit (Biorexfars, Iran). The ELISA reader was employed to measure absorbance at 405 nm.

### Quantitative real-time PCR (qPCR) analysis

hDPSCs and hDFs at a density of 3 × 10<sup>5</sup> cells were cultured in the 6-well plates. After reaching 70% confluence, the cells in the control group were treated with OM, while another group was exposed to HA-NPs without OM. RNA was isolated 14 days following osteogenic induction (19) using a kit (Pars Tous, Tehran, Iran). The cDNA Synthesis kit (Pars Tous, Tehran, Iran) was used to reverse transcribe a total extracted RNA into cDNA. After that, qPCR was carried out using a Real-Time PCR machine using the SYBR Green assay (Applied Biosystems). The relative expression of Bone morphogenetic protein-2 (BMP-2), Runt-related transcription factor 2 (RUNX2), Vascular endothelial growth factor-A (VEGF-A), and Interleukin-6 (IL-6) was determined using GAPDH as the internal reference gene. The primer sequences used are shown in Table 1.

**Table 1. Sequences of primers used for quantitative real-time PCR (qPCR)**

| Name          | Forward                   | Reverse                | Product length (bp) |
|---------------|---------------------------|------------------------|---------------------|
| <b>VEGF-A</b> | AGGGCAGAA TCATCACGA AGT   | AGGGTCTCGATT GGATGGCA  | 75                  |
| <b>RUNX2</b>  | ACCTTGACCATAACCGTCTTC     | GGCGGTCAGAGAACAACAACTA | 145                 |
| <b>BMP-2</b>  | GAGAAGGAGGAGGCAAAGAAAAG   | GAAGCAGCAACGCTAGAAGAC  | 183                 |
| <b>IL-6</b>   | AGACTTGCC TGGTGAAAA TCA   | GCTCTGGCTTGT TCCTCACT  | 100                 |
| <b>GAPDH</b>  | CGAACCTCTCTGCTCCTCCTGTTCG | CATGGTGTCTGAGCGATGTGG  | 83                  |

### Statistical analysis

GraphPad Prism software, Version 9 (GraphPad Software, Inc., La Jolla, CA), was used to do statistical analysis. A one-way analysis of variance (ANOVA) was used to discover significant differences between study groups, setting the statistical significance level at  $p < 0.05$ .

## Results

### Morphological characterization of HA-NPs

In a previous study, the morphological characterization of HA-NPs was conducted through the FESEM and TEM image analysis. The particles displayed a nanorod morphology with dimensions spanning from 17–29 nm in width and 62–89 nm in length (11).

### Determination of cell viability of HA-NPs treated hDPSCs and hDFs

The investigation involved assessing the cell viability of hDPSCs and hDFs treated with HA-NPs. The viability of hDPSCs and hDFs exposed to HA-NPs was evaluated at 24 and 72 hours using the MTT procedure (Figure 1).

The outcomes showed that HA-NP treated hDPSCs and hDFs at doses ranging from 5 to 100  $\mu\text{g/ml}$  did not show significant differences in cell toxicity or proliferation compared to the control group ( $p > 0.05$ ) after 24 and 72 hours. Consequently, the concentration of 100  $\mu\text{g/ml}$  was selected for subsequent experiments involving hDPSCs and hDFs.

### Determination of osteogenic differentiation of hDPSCs and hDF exposed to osteogenic and NPs media

Staining with ARS enabled the imagination of extracellular calcium accumulation, appearing as an orange-red color (Figure 2). The staining results indicated that hDPSCs and hDFs cultured in the control medium did not exhibit the formation of mineralized nodules.

However, after being cultured for 14 days in the presence of OM and HA-NP medium, both hDPSCs and hDFs developed dense, unequally distributed mineralized nodules. Quantitative analysis of ARS staining confirmed these findings, demonstrating a noticeably greater level of staining in hDPSCs compared to hDFs in both the OM media ( $p < 0.05$ ) and HA-NP media ( $p < 0.001$ ).

Furthermore, the level of staining on hDPSCs and hDFs cultured in the HA-NP medium was notably greater than that observed in the OM ( $p < 0.001$ ).

### Determination of ALP activity of hDPSCs and hDFs exposed to osteogenic and NPs media

Figure 3 depicts the ALP activity of hDPSCs and hDF exposed with osteogenic and NPs medium. alkaline phosphatase activity of hDPSCs and hDFs cultured in NP medium was notably higher than that in OM ( $p < 0.05$ ) and there was no significant difference in alkaline phosphatase activity when compared to hDPSCs and hDFs in the OM and NP media.

### Effects of HA-NPs on the expression of osteogenic markers detected by quantitative real-time PCR (qPCR)

hDPSCs and hDFs incubated with NP indicated up-regulation of BMP-2 expression levels ( $p<0.01$ ) at day 14, comparable to OM groups (hDF and hDPSC). There was no significant difference in the expression of BMP-2 observed between the hDPSC NP and hDF NP groups (Figure 4A). Incubation of hDFs and hDPSCs in NPs led to a notable decrease in RUNX2

gene expression ( $p<0.001$  and  $p<0.01$ , respectively) at day 14 (Figure 4B). The expression of IL-6 was notably increased in hDFs at 14 days of culture in the NPs group ( $p<0.01$ ). There was no significant difference in IL-6 expression observed between the hDPSC OM and hDPSC NP groups (Figure 4C). VEGF-A expression was increased in hDPSCs and hDFs cultured in NPs ( $p<0.05$ ). No significant difference in VEGF-A expression was observed in the hDPSC NP and hDF NP groups (Figure 4D).

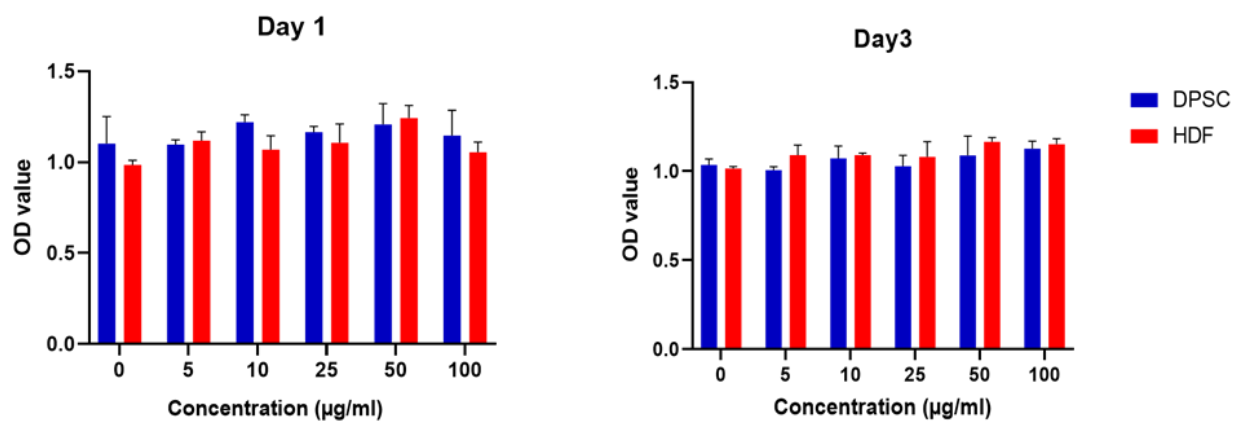


Figure 1. Viability assay for hDPSCs and hDFs incubated with HA-NPs on 24 and 72h.

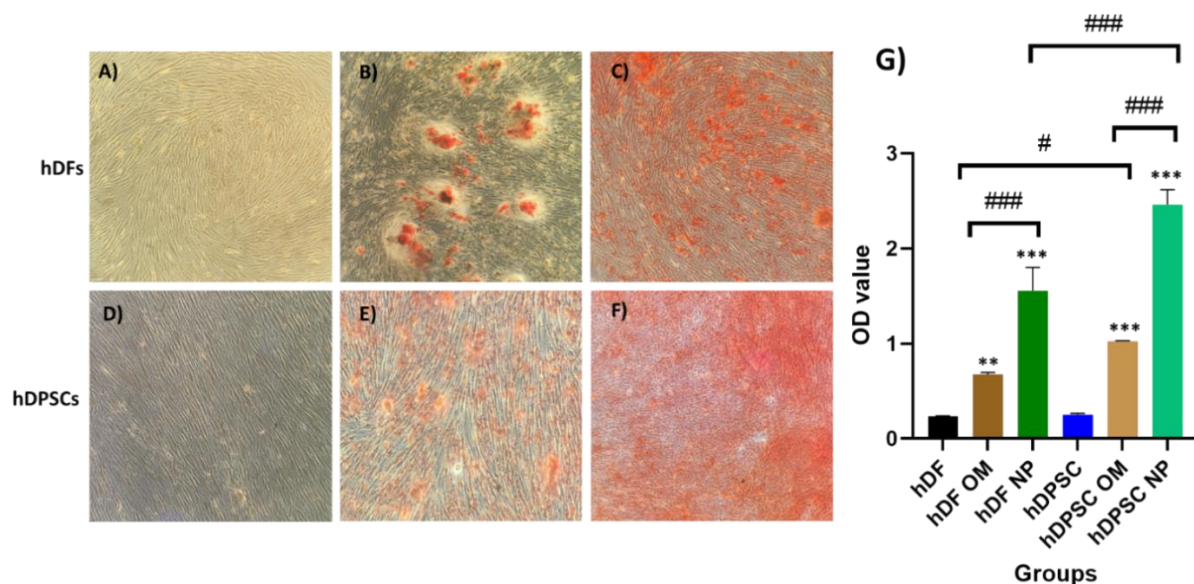
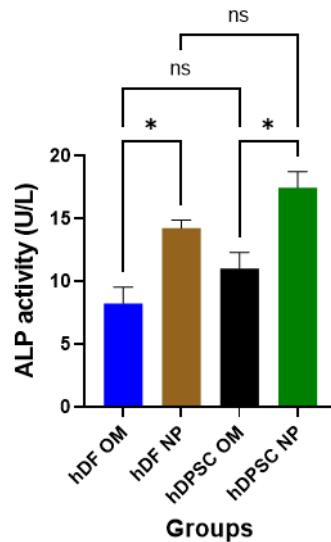
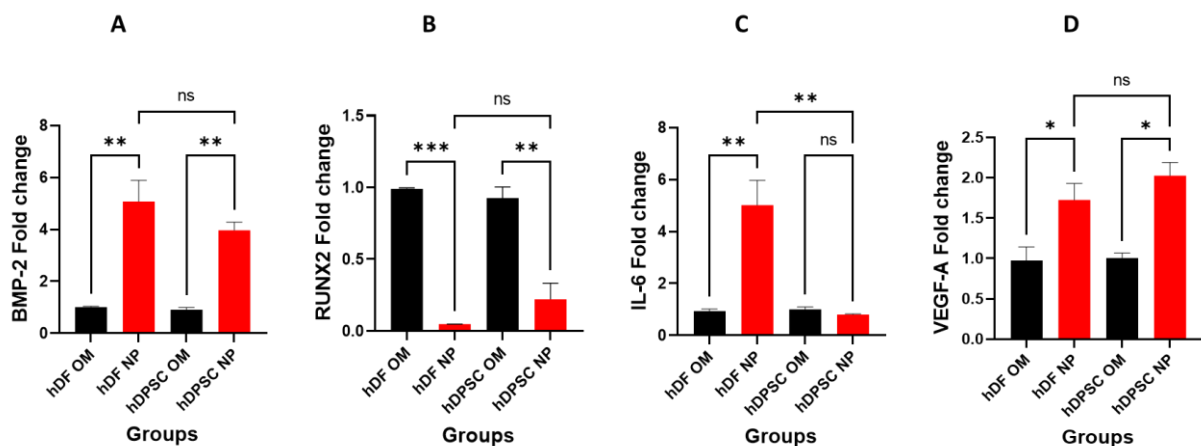


Figure 2. Microscopic views of Alizarin Red S staining of cultured hDPSCs and hDFs after 14 days in control medium (A&D), osteogenic medium (OM; B&E) and HA-NP medium (C&F). (G) A bar chart indicating the quantitative findings of differentiated hDPSCs and hDFs stained with alizarin red S after 14 days of culture.  $**p<0.01$ ;  $***p<0.001$  for each group compared to the control group.  $\square$  differences between groups.  $\#p<0.05$ ;  $###p<0.001$ . Abbreviations: hDPSC, human dental pulp stem cells; hDF, human dermal fibroblasts; OM, osteogenic medium, NP; nanoparticle



**Figure 3.** ALP activity of hDPSCs, and hDFs cultured for 14 days in OM and NP medium. \* $p < 0.05$  for each group compared to the control group. —; Differences between groups. Abbreviations: hDPSCs, human dental pulp stem cells; hDF, human dermal fibroblasts; OM, osteogenic medium; NP, nanoparticle; ns, nonsignificant



**Figure 4.** Gene expression levels of (A) BMP-2, (B) RUNX2, (C) IL-6, and (D) VEGF-A in cultured hDFs and hDPSCs for 14 days in the presence of OM and NP. \* $p < 0.05$ , \*\* $p < 0.01$ ; \*\*\* $p < 0.001$  for each group compared to the control group. —; differences between groups. Abbreviations: hDPSC, human dental pulp stem cells; hDF, human dermal fibroblasts; OM, osteogenic medium; NP, nanoparticle; ns, nonsignificant.

## Discussion

This study evaluated the osteogenic differentiation capacity of hDPSCs and hDFs in the presence of HA-NPs. HA-NPs, due to their strong structural similarity to natural bone minerals, serve a vital role in promoting remineralization and accelerating bone production, which are crucial steps for successful bone regeneration (20). Previous studies have highlighted the remarkable biocompatibility and outstanding bone

regeneration capabilities of HA-based composites (21). These findings highlight HA-NPs' potential as a biomaterial that holds promise for developing regenerative therapies in bone tissue engineering. Considering the results of this study, the cell viability assay indicated that HA-NPs, had no harmful effect on hDFs and hDPSCs up to 100  $\mu\text{g/ml}$ . In this regard, Shahoon et al. found no toxicity in L929 fibroblast cells at any tested concentrations of HA-NPs. Although cell viability decreased with higher HA-NPs concentration

and duration of exposure, the groups did not show statistically significant variance (22). Additionally, our previous study demonstrated that HA-NPs significantly decreased the viability of DPSCs at 500 and 1000 µg/ml compared to the control group (11).

Two main ingredients of HA are calcium and phosphate. The level of HA-NP-induced cell death is strongly correlated with the particle dosage. To increase intracellular  $\text{Ca}^{2+}$  concentrations, the HA-NPs is broken down in cell lysosomes, potentially causing lysosomal rupture and necrosis of the cell. Furthermore, large amounts of HA-NPs may cause mechanical harm to cells and consequent sedimentation, which can lead to cytotoxicity (19). ARS staining primarily employs ARS to react with calcium nodules produced in osteogenic-stimulated extracellular, leading to rich red compounds that can indicate the osteogenic differentiation potential of cells (23). Monterubbianesi et al. showed that the differentiating ability of fibroblast cells varies depending on their source. Furthermore, compared to hDPSCs, calcium deposits are substantially lower (8). The results of ARS staining in our study showed that hDPSCs contained more mineral-containing vesicles and more mineralized nodules. Consequently, hDPSCs exhibit greater osteogenic differentiation potential in comparison to hDFs.

The assessment of ALP activity serves as an essential parameter in considering the osteogenic differentiation potential of cells (18). During the process of osteoblast differentiation, ALP is produced and serves as an early indicator of bone formation and osteoblast, providing insight into the biological activity of osteoblasts (23).

Hee et al. showed that human dermal fibroblasts may produce a noticeable ALP activity at 21 days when an appropriate ossifying material is present (12). Our outcomes demonstrated that HA-NPs might encourage the development of osteoblasts in hDFs as well as hDPSCs. Furthermore, it was shown that there is no difference in ALP activity between hDFs and hDPSCs. BMP-2, RUNX2, VEGF-A, and IL-6 are well-known indicators of osteogenesis and regeneration. BMP-2, a member of the TGF- $\beta$  superfamily, is well known for its potent capability to promote bone formation and regeneration. It is the most important and widely used bone growth factor because it promotes osteogenic healing by boosting the early abundance of osteogenic precursor cells at the site of bone injury, as well as their

differentiation and mineralization into mature osteoblasts (24). Moreover, BMP-2, is the most potent osteoinductor, promoting the development of MSCs into osteoblasts (25). We used qPCR to confirm whether NPs stimulating bone formation increase BMP-2 expression to confirm the above data. Our result showed that culture in osteogenic media with NPs can increase the level of BMP-2 expression on day 14. According to previous study results, RUNX2 serves as an important function in promoting the initial differentiation of osteoblasts and is considered a key transcription factor for the development of skeletal and tooth structures. Its influence is most prominent during the early phases of odontogenic differentiation and is downregulated as differentiation progresses (23, 26). RUNX2 directs the production of juvenile bone by inducing multipotent mesenchymal cells to differentiate into immature osteoblasts, but it also suppresses osteoblast maturation and mature bone development. Typically, the protein level of RUNX2 in osteoblasts decreases throughout bone development, and osteoblasts have mature phenotypes, which are essential for mature bone production (27).

According to research by Monterubbianesi et al., fibroblasts and hDPSCs grown in OM showed elevated RUNX2 expression on day 7, which was followed by a decrease on day 14 (8). Similarly, another study had shown that mRNA levels of RUNX2 in hDPSCs rose in response to growth on mesoporous bioactive glass nanoparticle/graphene oxide composites on day 7 and declined on day 14. Consistently, our results demonstrated reduced RUNX2 levels in hDPSCs and hDFs cultured with NPs on day 14.

Aside from prompting bone stimulation, angiogenesis is crucial for effective bone regeneration. Angiogenesis is the development of new blood vessels from an existing vascular network. These newly created vessels are vital for supplying nutrients, transporting macromolecules, allowing cell invasion, and maintaining the necessary metabolic balance during bone healing.

The vascular endothelial growth factor (VEGF) is recognized as a crucial regulator of angiogenesis in the process of bone formation (28). The critical significance of VEGF in bone regeneration has been proven in different experimental models of bone formation. These models exhibit the enhancement or hindrance of typical fracture healing or the formation of bone in vivo following the administration or

inhibition of VEGF, respectively (29-32). VEGF is essential for intramembranous ossification in addition to promoting vascular invasion and the recruitment of cartilage fragment tissues to hypertrophic cartilage. Thus, the proper physiological function of bone depends on the close relationship between angiogenesis and osteogenesis (23). DPSCs exhibit phenotypes consistent with perivascular cell populations and contribute to the processes of vasculogenesis and angiogenesis by releasing pro-angiogenesis factors like VEGF (33).

According to our study, after two weeks in osteogenic conditions, VEGF-A expression increased in both hDPSCs and hDFs. IL-6 is a multifunctional immune cytokine that is produced and released by osteoblast cell lines and osteoclasts. It is required for optimal bone formation and regeneration (34). It has been shown that IL-6 promotes the osteogenic development of BMSCs by activating the STAT3 signaling pathway in the context of bone metabolism (35). Additionally, it contributes to the promotion of the osteogenic differentiation process of preosteoblasts and adipose stem cells (36).

Huh et al. also indicated that adipose MSCs can secrete IL-6 in response to Toll-like receptor activation, which encourages the osteogenic differentiation of adipose-derived MSCs (37). Furthermore, IL-6 controls osteoblast and osteoclast differentiation and triggers the production of vascular endothelial growth factor to encourage vascularization (34). All of the aforementioned studies indicate that IL-6 is pivotal in facilitating the regeneration of bones. The findings evince a conspicuous absence of discernible alterations in the expression profile of IL-6 in hDPSCs subsequent to a 14-day treatment of NP media. However, our previous study showed that an increase in IL-6 levels occurs in 24-hour treatment with NPs (11).

Additionally, it was discovered that in NPs media, the expression level of IL-6 increased in hDFs. This study demonstrates that HA-NPs have the ability to improve the osteogenic properties of hDPSCs and hDFs. Exposure to HA-NPs enhanced the osteogenic potential of both hDPSCs and hDFs, as evidenced by increased ARS staining for calcium deposition and elevated ALP activity. While both cell types show some mineralization potential, hDPSCs are more advantageous for bone regeneration applications,

emphasizing their suitability in regenerative medicine strategies.

## Acknowledgements

The authors would like to thank the Birjand University of Medical Sciences. Birjand University of Medical Sciences provided support for this study (Approval ID: IR.BUMS.REC.1403.011, Grant No: 6544).

## References

1. Peng Y, Qu R, Feng Y, et al. Regulation of the integrin  $\alpha$ V $\beta$ 3-actin filaments axis in early osteogenesis of human fibroblasts under cyclic tensile stress. *Stem Cell Res Ther.* 2021;12(1):1-12.
2. Hefka Blahnová V, Vojtová L, Pavlíňáková V, et al. Calcined hydroxyapatite with collagen I foam promotes human MSC osteogenic differentiation. *Int J Mol Sci.* 2022;23(8):4236.
3. Black CR, Goriainov V, Gibbs D, et al. Bone tissue engineering. *Curr Mol Biol Rep.* 2015;1(3):132-40.
4. Leyendecker Junior A, Gomes Pinheiro CC, Lazzaretti Fernandes T, et al. The use of human dental pulp stem cells for in vivo bone tissue engineering: a systematic review. *J Tissue Eng.* 2018;9:2041731417752766.
5. Ressler A, Žužić A, Ivanišević I, et al. Ionic substituted hydroxyapatite for bone regeneration applications: A review. *Open Ceramics.* 2021;6:100122.
6. Huang H, Qiang L, Fan M, et al. 3D-printed tri-element-doped hydroxyapatite/polycaprolactone composite scaffolds with antibacterial potential for osteosarcoma therapy and bone regeneration. *2024;3:118-37.*
7. Shi H, Zhou Z, Li W, et al. Hydroxyapatite based materials for bone tissue engineering: A brief and comprehensive introduction. *Crystals.* 2021;11(2):149.
8. Monterubbianesi R, Bencun M, Pagella P, et al. A comparative in vitro study of the osteogenic and adipogenic potential of human dental pulp stem cells, gingival fibroblasts and foreskin fibroblasts. *Sci Rep.* 2019;9(1):1761.
9. Cui Y, Ji W, Gao Y, et al. Single-cell characterization of monolayer cultured human



- dental pulp stem cells with enhanced differentiation capacity. *Int J Oral Sci.* 2021;13(1):44.
10. Tsutsui TW. Dental Pulp Stem Cells: Advances to Applications. *Stem Cells Cloning.* 2020;13:33-42.
  11. Azaryan E, Mortazavi-Derazkola S, Alemzadeh E, et al. Effects of hydroxyapatite nanorods prepared through *Elaeagnus Angustifolia* extract on modulating immunomodulatory/dentin-pulp regeneration genes in DPSCs. *Odontology.* 2023;111(2):461-73.
  12. Hee CK, Jonikas MA, Nicoll SBJB. Influence of three-dimensional scaffold on the expression of osteogenic differentiation markers by human dermal fibroblasts. *Biomaterials.* 2006;27(6):875-84.
  13. Claeys L, Bravenboer N, Eekhoff EM, et al. Human fibroblasts as a model for the study of bone disorders. *Front Endocrinol (Lausanne).* 2020;11:394.
  14. Lv F-J, Tuan RS, Cheung KM, et al. Concise review: the surface markers and identity of human mesenchymal stem cells. *Stem Cells Int.* 2014;32(6):1408-19.
  15. Haniffa MA, Wang X-N, Holtick U, et al. Adult human fibroblasts are potent immunoregulatory cells and functionally equivalent to mesenchymal stem cells. *J Immunol.* 2007;179(3):1595-604.
  16. Saharkhiz M, Ayadilord M, Emadian Razavi F, et al. Effects of phytosomal curcumin treatment on modulation of immunomodulatory and pulp regeneration genes in dental pulp mesenchymal stem cells. *Odontology.* 2022;110(2):287-95.
  17. Azaryan E, Hanafi-Bojd MY, Alemzadeh E, et al. Effect of PCL/nHAEA nanocomposite to osteo/odontogenic differentiation of dental pulp stem cells. *BMC Oral Health.* 2022;22(1):505.
  18. Hokmabad VR, Davaran S, Aghazadeh M, et al. Effect of incorporating *Elaeagnus angustifolia* extract in PCL-PEG-PCL nanofibers for bone tissue engineering. *Front Chem Sci Eng.* 2019;13:108-19.
  19. Yang X, Li Y, Liu X, et al. In vitro uptake of hydroxyapatite nanoparticles and their effect on osteogenic differentiation of human mesenchymal stem cells. *Stem Cells Int.* 2018;2018(1):2036176.
  20. Hoveidaei AH, Sadat-Shojai M, Mosalamiaghili S, et al. Nano-hydroxyapatite structures for bone regenerative medicine: Cell-material interaction. *Bone.* 2024;179:116956.
  21. Fang C-H, Lin Y-W, Lin F-H, et al. Biomimetic synthesis of nanocrystalline hydroxyapatite composites: Therapeutic potential and effects on bone regeneration. *Int J Mol Sci.* 2019;20(23):6002.
  22. Shahoon H, Hamed R, Yadegari Z, et al. The comparison of silver and hydroxyapatite nanoparticles biocompatibility on L929 fibroblast cells: an. *J Nanomed Nanotechnol.* 2013;4(4):1000173.
  23. Chen X, Gao C-Y, Chu X-Y, et al. VEGF-loaded heparinised gelatine-hydroxyapatite-tricalcium phosphate scaffold accelerates bone regeneration via enhancing osteogenesis-angiogenesis coupling. *Front Bioeng Biotechnol.* 2022;10:915181.
  24. Zhao L, Zhao X, Deng F, et al. Integration of BMP-2/PLGA microspheres with the 3D printed PLGA/CaSO<sub>4</sub> scaffold enhances bone regeneration. *Front Mater.* 2024;11:1374409.
  25. Nedorubova IA, Bukharova TB, Mokrousova VO, et al. Comparative efficiency of gene-activated matrices based on chitosan hydrogel and PRP impregnated with BMP2 polyplexes for bone regeneration. *Int J Mol Sci.* 2022;23(23):14720.
  26. Ahn JH, Kim I-R, Kim Y, et al. The effect of mesoporous bioactive glass nanoparticles/graphene oxide composites on the differentiation and mineralization of human dental pulp stem cells. *Nanomaterials (Basel).* 2020;10(4):620.
  27. Komori T. Regulation of osteoblast differentiation by Runx2. *Adv Exp Med Biol.* 2010;658:43-9.
  28. Kempen DH, Lu L, Heijink A, et al. Effect of local sequential VEGF and BMP-2 delivery on ectopic and orthotopic bone regeneration. *Biomaterials.* 2009;30(14):2816-25.
  29. Eckardt H, Ding M, Lind M, et al. Recombinant human vascular endothelial growth factor enhances bone healing in an experimental nonunion model. *J Bone Joint Surg Br.* 2005;87(10):1434-8.
  30. Kaigler D, Wang Z, Horger K, et al. VEGF scaffolds enhance angiogenesis and bone regeneration in irradiated osseous defects. *J Bone Miner Res.* 2006;21(5):735-44.
  31. Peng H, Usas A, Olshanski A, et al. VEGF improves, whereas sFlt1 inhibits, BMP2-induced bone formation and bone healing through modulation of angiogenesis. *J Bone Miner Res.* 2005;20(11):2017-27.

32. Street J, Bao M, deGuzman L, et al. Vascular endothelial growth factor stimulates bone repair by promoting angiogenesis and bone turnover. *Proc Natl Acad Sci U S A*. 2002;99(15):9656-61.
33. Mattei V, Martellucci S, Pulcini F, et al. Regenerative potential of DPSCs and revascularization: direct, paracrine or autocrine effect? *Stem Cell Rev Rep*. 2021;17(5):1635-46.
34. Yang N, Liu YJJoMS. The role of the immune microenvironment in bone regeneration. *Int J Med Sci*. 2021;18(16):3697-707.
35. Xie Z, Tang Sa, Ye G, et al. Interleukin-6/interleukin-6 receptor complex promotes osteogenic differentiation of bone marrow-derived mesenchymal stem cells. *Stem Cell Res Ther*. 2018;9(1):1-10.
36. Bastidas-Coral AP, Bakker AD, Zandieh-Doulabi B, et al. Cytokines TNF $\alpha$ , IL $\beta$ 6, IL $\beta$ 17F, and IL $\beta$ 4 differentially affect osteogenic differentiation of human adipose stem cells. *Stem Cells Int*. 2016;2016(1):1318256.
37. Huh J-E, Lee SYJBeBA-MCR. IL-6 is produced by adipose-derived stromal cells and promotes osteogenesis. *Biochim Biophys Acta*. 2013;1833(12):2608-16.